Magnetocaloric and magnetotransport properties of R_2Ni_2Sn compounds (R=Ce, Nd, Sm, Gd, and Tb)

Pramod Kumar,[1,2] Niraj K. Singh,[1,*] K. G. Suresh,[1,†] and A. K. Nigam[3]
[1]*Department of Physics, IIT Bombay, Mumbai 400076, India*
[2]*Institut fuer Metallische Werkstoffe, Helmholtz Strasse 20, D-01069 Dresden, Germany*
[3]*Tata Institute of Fundamental Research, Homi Bhabha Road, Mumbai 400005, India*
(Received 27 December 2007; revised manuscript received 9 March 2008; published 12 May 2008)

We report a detailed magnetic, magnetocaloric, and magnetotransport study on R_2Ni_2Sn compounds with different rare earths. The magnetic state of these compounds is found to be complex because of the coexistence of ferromagnetic and antiferromagnetic components. These compounds show phenomena such as multiple magnetic transitions, nonsaturation of magnetization, and metamagnetic transitions. Analysis of the zero-field heat capacity data shows that the magnetic entropy is less than the theoretical value, indicating the presence of some moment on Ni. Schottky anomaly is present in the magnetic heat capacity data of Sm_2Ni_2Sn. The temperature variation of magnetocaloric effect reflects the magnetization behavior. Tb_2Ni_2Sn and to a less extent Gd_2Ni_2Sn show oscillatory magnetocaloric effect. The variation of magnetocaloric effect is correlated with the ferromagnetic-antiferromagnetic phase coexistence. The electrical resistivity analysis has shown that the electron-magnon scattering is prominent at low temperature, while phonon scattering modified by the *s-d* interaction is crucial at high temperatures. The magnetoresistance is very large in Ce_2Ni_2Sn and shows a quadratic dependence on the field, implying the role of spin fluctuations in determining the transport behavior. Large magnetoresistance has been observed in other compounds as well.

DOI: 10.1103/PhysRevB.77.184411 PACS number(s): 71.20.Eh, 75.30.Sg, 75.30.Kz

I. INTRODUCTION

Magnetocaloric effect (MCE) is an intrinsic property of magnetic solids and it arises due to the coupling of the magnetic sublattice with the magnetic field.[1–8] MCE can be measured in terms of isothermal magnetic entropy change (ΔS_M) or adiabatic temperature change (ΔT_{ad}). In ferromagnets, the entropy change during isothermal magnetization is negative and it is termed as positive MCE. On the other hand, there are some substances that exhibit negative MCE, i.e., the entropy change is positive. Generally, this occurs in antiferromagnetic (AFM) materials, in which the applied magnetic field increases the magnetic entropy. Materials with positive MCE are being considered as active materials in magnetic refrigerators, whereas the ones with negative MCE would find applications in heat pumps.[3]

The search for potential working substances suitable for cooling in the "sub-room-temperature" and "near room temperature" regimes is essential for the future development of magnetic refrigeration technology. Materials with first-order magnetic transition are of particular interest since they exhibit significant values of the isothermal magnetic entropy change and the adiabatic temperature change at the magnetic transition temperature. This is because the magnitude of MCE critically depends on the first derivative of the magnetization with respect to the temperature. Compounds showing field-induced magnetic transitions and/or structural transitions have been found to exhibit very large MCE, as in the case of $Gd_5Si_2Ge_2$.[9–11] Giant magnetocaloric effect was also found in $LaFe_{11.4}Si_{1.6}$,[12] MnAs,[13,14] FePMnAs,[15] RCo_2,[16,17] Heusler alloys,[18] manganites,[19] etc. In most of these cases, the giant MCE is a result of a first-order ferromagnetic (FM) to paramagnetic transition. Another material system that will be of interest in the field of MCE is the one which shows multiple magnetic transitions. This is because of the possibility of achieving "tablelike" MCE over a considerable temperature regime.

The variety of magnetic phenomena exhibited by many rare earth (R)–transition metal (TM) intermetallic compounds renders them superior candidates for applications based on MCE. Among the R-TM intermetallics, R_2Ni_2Sn compounds remain unexplored with respect to their magnetocaloric behavior. Many compounds of this series show multiple magnetic transitions, which may be exploited for obtaining "tablelike MCE." Though basic structural, magnetic, and transport studies have been reported in most of these compounds,[20–27] there are no detailed investigations on their heat capacity behavior as well. Similarly, this series has not been subjected to a detailed magnetotransport study. These compounds crystallize in the orthorhombic W_2CoB_2-type structure. Since the Ni sublattice is almost nonmagnetic in these compounds, the magnetic structure is determined mainly by the RKKY interaction and the crystalline electric fields (CEFs), which determine the ground state of the R ion. The oscillatory character of the RKKY interaction leads to the occurrence of commensurate or incommensurate magnetic structures. CEF effects may cause anisotropic exchange interactions, which may also play a role in determining the magnetic state. With the objective of establishing the correlations among the magnetic, magnetothermal, and magnetotransport properties of these compounds, we have studied the magnetocaloric effect and the magnetoresistance (MR) in polycrystalline R_2Ni_2Sn [R=Ce, Nd, Sm, Gd, and Tb] compounds, and the results are presented in this paper.

II. EXPERIMENTAL DETAILS

Polycrystalline samples of R_2Ni_2Sn with R=Ce, Nd, Sm, Gd, and Tb were synthesized by arc melting. The purity of

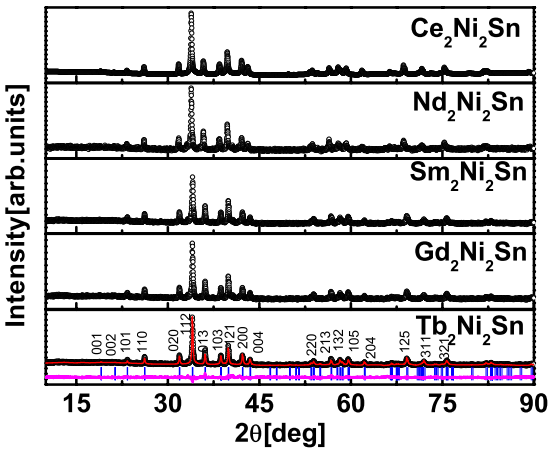

FIG. 1. (Color online) Rietveld refined powder x-ray diffractograms of R_2Ni_2Sn compounds. The plot at the bottom in the case of Tb_2Ni_2Sn shows the difference between the experimental and calculated intensities.

the starting elements was 99.9% for the rare earths and 99.99% for Ni and Sn. The ingots were melted several times to ensure homogeneity. The as-cast samples were annealed under vacuum at 800 °C for 3 weeks. The phase purity was checked by the Rietveld refinement of the powder x-ray diffraction (XRD) data and energy dispersive analysis of x-ray (EDAX) facility attached to a scanning electron microscope. The magnetization (M) measurements, both under "zero-field-cooled" (ZFC) and "field-cooled worming" (FCW) conditions, in the temperature (T) range of 5–220 K and up to a maximum field (H) of 100 kOe were performed by using a vibrating sample magnetometer (Oxford). The heat capacity (C) and electrical resistivity (ρ) were measured in the temperature range of 2–280 K and in fields up to 90 kOe by using a physical property measurement system (Quantum Design). The magnetocaloric effect has been calculated both in terms of isothermal magnetic entropy change and adiabatic temperature change by using the heat capacity data in zero field and at different fields, as well as using the M-H-T data.

III. RESULTS AND DISCUSSION

The Rietveld refined XRD patterns of these compounds at room temperature are shown in Fig. 1. The typical difference plot obtained between the experimental and the calculated intensities is given at the bottom for Tb_2Ni_2Sn. Similar difference plots were obtained in other compounds as well. Based on this, it is clear that all the compounds have formed in single phase with the W_2CoB_2-type orthorhombic structure (space group=*Immm*). The phase purity of these compounds was also analyzed with the help of EDAX method. It was found that a 2:2:1 composition was present uniformly over the sample surface. Therefore, XRD and EDAX analyses suggest that the impurities, if any, are quite negligible. The lattice parameters obtained from the Rietveld refinement are given in the Table I. These values are in good agreement with those reported in literature.[21–24] The regular decrease of the lattice volume with increasing rare earth atomic number reflects the lanthanide contraction. It is found that $d_{\text{Ni-Sn}}$ bond length varies from 2.734 to 2.665 Å following the sequence of Ce_2Ni_2Sn to Tb_2Ni_2Sn. These values, much smaller than the sum of the metallic radii ($r_{\text{Ni}}+r_{\text{Sn}}=2.869$ Å), suggest a strong overlap between the $3d$ (Ni)–$5p$ (Sn) orbitals.

The M vs T plots of these compounds, which are obtained in an applied field of 500 Oe under ZFC and FCW modes, are shown in Figs. 2(a)–2(e). It is clear from the FCW data that while Sm_2Ni_2Sn and Gd_2Ni_2Sn are ferromagnetic, the others are antiferromagnetic at low temperatures. Furthermore, it can be seen that these compounds, except Ce_2Ni_2Sn, exhibit considerable thermomagnetic irreversibility, which is attributed to the pinning of domain walls. There may be a contribution from the complex magnetic structure as well, which causes the thermomagnetic irreversibility.[28,29] In Gd_2Ni_2Sn, the thermomagnetic irreversibility is found to be very small, which is due to the weak magnetic anisotropy associated with Gd^{3+} ion. Since the domain wall pinning effect is quite prominent in materials with large magnetic anisotropy, negligible thermomagnetic irreversibility seen in Gd_2Ni_2Sn implies that at least in this compound, the domain wall pinning is the dominant factor in contributing the thermomagnetic irreversibility.

Another observation from the M-T plots is the signature of multiple magnetic transitions in Nd_2Ni_2Sn, Sm_2Ni_2Sn, Nd_2Ni_2Sn, and Tb_2Ni_2Sn. It is clear from Fig. 2 that there are two magnetic transitions in Nd_2Ni_2Sn (at 17 and 22 K) and three transitions in Sm_2Ni_2Sn (at 15, 21, and 52 K) and Tb_2Ni_2Sn (at 8, 42, and 66 K). The magnetic transition temperatures are designated as T_1, T_2, and T_3 in decreasing order. The transition temperatures represent T_C or T_N, depending on whether the transition is ferromagnetic-paramagnetic or antiferromagnetic-paramagnetic in nature. The transition

TABLE I. Lattice parameters, unit cell volume, and R-Ni and R-R bond lengths in R_2Ni_2Sn compounds.

Compound	a (Å)	b (Å)	c (Å)	V (Å^3)	$d_{\text{Ni-Sn}}$ (Å)	$d_{R\text{-}R}$ (Å)
Ce_2Ni_2Sn	4.391(2)	5.730(3)	8.586(4)	216.027	2.734	3.642
Nd_2Ni_2Sn	4.362(2)	5.701(3)	8.503(5)	211.439	2.715	3.607
Sm_2Ni_2Sn	4.321(3)	5.670(3)	8.418(4)	207.027	2.693	3.571
Gd_2Ni_2Sn	4.291(3)	5.632(4)	8.391(7)	202.785	2.671	3.560
Tb_2Ni_2Sn	4.277(3)	5.609(4)	8.323(5)	199.647	2.665	3.531

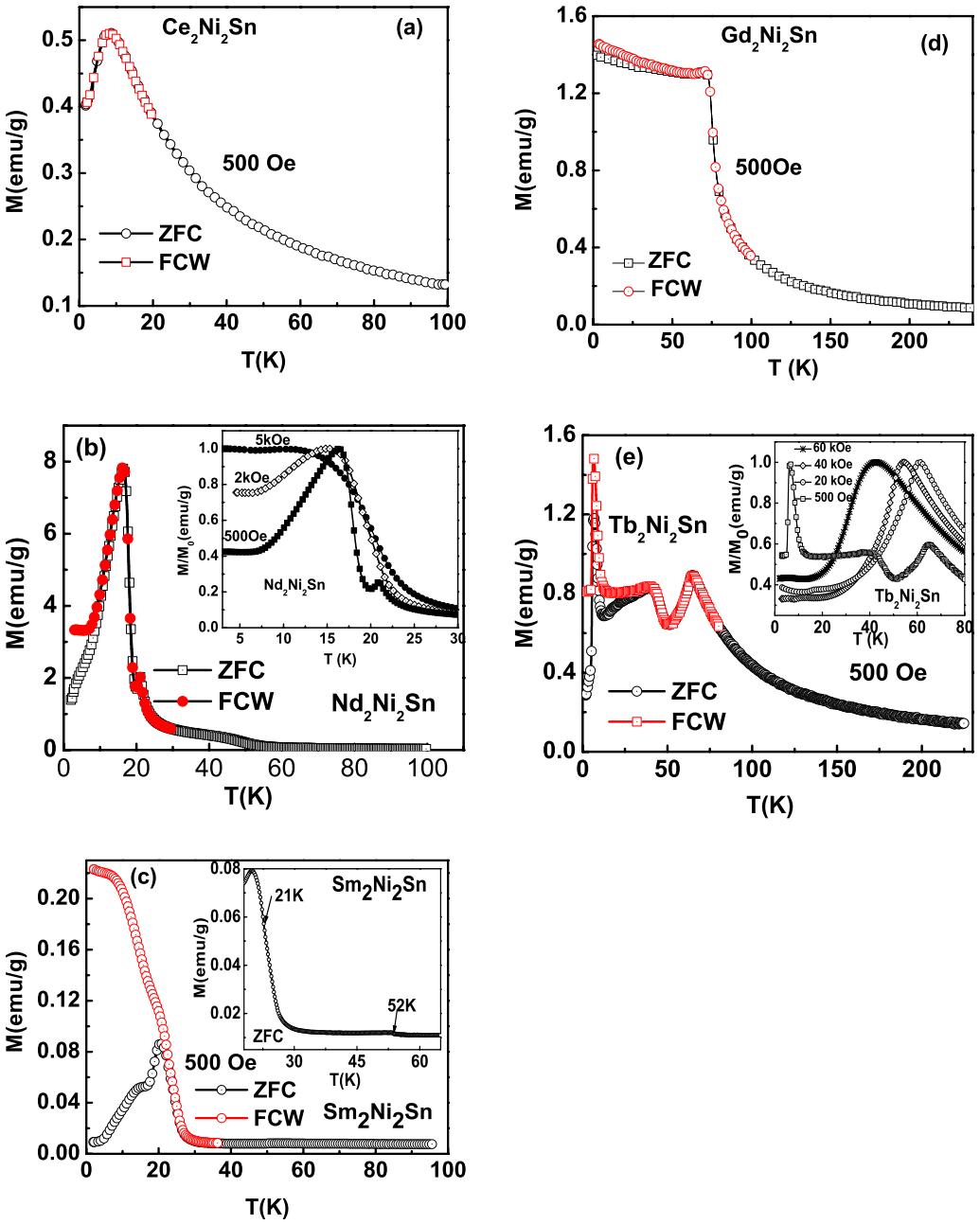

FIG. 2. (Color online) Temperature dependence of magnetization of (a) Ce_2Ni_2Sn, (b) Nd_2Ni_2Sn, (c) Sm_2Ni_2Sn, (d) Gd_2Ni_2Sn, and (e) Tb_2Ni_2Sn obtained under 500 Oe, both under ZFC and FCW modes. The insets of (b) and (e) show the temperature dependence of magnetization at higher fields. The inset of (c) shows the expanded low temperature region.

temperatures for all the compounds, which are obtained by plotting the first derivative (dM/dT), are given in Table II.

To further understand the nature of magnetic transitions, M-T data were collected at higher fields, i.e., $H=2$ and 5 kOe in the case of Nd_2Ni_2Sn [shown in the inset of Fig. 2(b)] and $H=20$, 40, and 60 kOe in the case of Tb_2Ni_2Sn [shown in the inset of Fig. 2(e)]. In the case of Nd_2Ni_2Sn, with an increase in field, the transition at 22 K disappears, while the one at 17 K shifts toward higher temperature. Therefore, the major transition is of ferromagnetic type with $T_C=17$ K. In Tb_2Ni_2Sn, the transitions at 8 and 42 K vanish at high fields, while the transition at 66 K shifts to lower temperatures. This implies that in Tb_2Ni_2Sn, $T_1=66$ K actually represents T_N. It is reasonable to infer that the predominant component at low temperatures in Tb_2Ni_2Sn is antiferromagnetic. The present observations in the case of Nd_2Ni_2Sn are in agreement with those reported by Chevalier *et al.*[23] It has been reported that Dy_2Ni_2Sn shows a behavior similar to that of Tb_2Ni_2Sn.[21] Furthermore, in general, the transition temperatures obtained in all these compounds are in very good agreement with earlier reports.[20–27]

The dc magnetic susceptibility at temperatures above the transition temperature T_1 is found to obey the Curie–Weiss law. The effective moment (μ_{eff}) and the paramagnetic Curie temperature (θ_p) obtained from the fit are given in Table II. It is evident from this table that the paramagnetic moment is

TABLE II. Magnetic transition temperatures, paramagnetic Curie temperature, experimental and theoretical saturation moments, calculated and theoretical effective moments, and temperature corresponding to the heat capacity peak (T^*) in R_2Ni_2Sn compounds.

Compound	T_1 (K)	T_2 (K)	T_3 (K)	θ_P (K)	M_s (μ_B/R^{3+}) 5 K	gJ (μ_B/R^{3+})	μ_{eff} (μ_B/R^{3+})	$g\sqrt{J(J+1)}$ (μ_B/R^{3+})	T^* (K)
Ce_2Ni_2Sn	8			10		0.8	2.5	2.5	
Nd_2Ni_2Sn	22	17		20	2.2	3.3	3.7	3.6	19
Sm_2Ni_2Sn	52	21	15	19			0.7	0.8	50
Gd_2Ni_2Sn	75			57	6.9	7	8.3	7.9	72
Tb_2Ni_2Sn	66	42	8	−39	8.2	9	10.9	9.7	61

slightly larger than the free ion moment of R^{3+} in most of the cases, which may be due to the small moments on Ni. Though it has been reported that Ni is almost nonmagnetic in these compounds, it may get an induced moment. It has been reported that in many compounds, Ni sublattice is found to get a small induced moment due to the strong molecular field of the rare earths. A similar observation has been reported in many Ni-based intermetallics.[28,29] Another important observation from the Curie–Weiss fit is that except Tb_2Ni_2Sn, in all the compounds, the sign of θ_p is positive. In compounds such as Ce_2Ni_2Sn and Nd_2Ni_2Sn, positive θ_p is not expected in view of the M-T data. These observations point to the fact that the magnetic structure of these compounds is not simple collinear type, but a more complex one. The complex nature arises due to the competing ferromagnetic and antiferromagnetic exchange interactions.[28,29] Like the transition temperatures, the values of μ_{eff} and θ_p obtained in the present case are also in agreement with the earlier reports.[21,22,27]

Figures 3(a)–3(e) show the field dependence of magnetization isotherms obtained at 5 K. The insets in the case Figs. 3(b)–3(e) show the isotherms at temperatures close to the magnetic transition temperatures. It can be seen from the figure that at 5 K, none of the compounds shows the complete saturation even at the highest field. Though all the compounds of this series crystallize in the same structure, their nonsaturation tendency is quite different. The nonsaturation in Ce_2Ni_2Sn is expected since its ordering temperature is only 8 K. The saturation trend is better in the case of Gd and Tb compounds compared to that of Nd_2Ni_2Sn. The scenario in Sm_2Ni_2Sn is far away from saturation. The saturation magnetization (M_s) values (per single rare earth ion) for Nd, Gd, and Tb compounds have been determined by plotting M vs $1/H$ plots and are listed in Table II. The M_s values of Nd_2Ni_2Sn, Gd_2Ni_2Sn, and Tb_2Ni_2Sn are found to be 2.2, 6.9, and 8.2μ_B, respectively. By comparing these values with the theoretical saturation moments (gJ) given in Table II, it is clear that Nd and Tb compounds are well below their saturation. The low saturation values seen in the present compounds may be attributed to the presence of a canted magnetic structure at low temperatures and/or the influence of the crystalline electric fields. However, since Gd compound is almost fully saturated, the role of crystal fields in the nonsaturation seems to be very nominal. It can be seen from these figures that apart from the nonsaturation tendency, metamagnetic transitions are present in Gd and Tb compounds. The critical fields needed for the metamagnetic transition in Gd and Tb compounds are ~40 and 65 kOe, respectively. It is surprising to note that Gd_2Ni_2Sn, whose M-T behavior was of ferromagnetic nature, also shows a metamagnetic transition. Therefore, it is clear that the magnetic state of this compound is not a simple collinear ferromagnetic type at low temperatures. The metamagnetic transition seen in these compounds may be attributed to the field-induced transition from antiferromagnetic or canted ferromagnetic state to a nearly collinear ferromagnetic state. By using neutron diffraction data, Penc *et al.*[21] showed that both Nd_2Ni_2Sn and Dy_2Ni_2Sn possess noncollinear magnetic structures at low temperatures. It may be mentioned here that such a field-induced transition from an antiferromagnetic to ferromagnetic state was reported in many materials.[30]

The M-H isotherms have been obtained at higher temperatures for all the compounds, except Ce_2Ni_2Sn. It can be seen from the inset of Fig. 3(b) that the isotherms of Nd_2Ni_2Sn, which are obtained in the temperature range of 10–40 K, do not show any metamagnetic transition. Sm_2Ni_2Sn shows a metamagnetic transition at 7 K, as evident from the inset of Fig. 3(c). At low fields, the magnetization increases with increase in temperature, whereas the trend reverses at high fields. A similar behavior is observed in Tb_2Ni_2Sn as well. Metamagnetic transition is also observed in Gd_2Ni_2Sn. Therefore, it is clear that the strength of the antiferromagnetic component is very small in Nd_2Ni_2Sn, while the magnetic state is predominantly antiferromagnetic below a certain field in the case of Gd and Tb compounds.

In order to further probe the nature of the magnetic state in these compounds, the heat capacity measurements were performed, both under zero field and in various fields. Figure 4 shows the temperature variation of heat capacity of R_2Ni_2Sn compounds in zero field. All of the compounds show λ-type anomaly at a temperature designated as T^*, which is close to the transition temperature T_1 in most of the cases. In the case of Nd_2Ni_2Sn, T^* is found to coincide with T_2. The nature of the peak implies that the magnetic transition at these temperatures is of second order. With increasing magnetic field, the peak becomes broader and shifts to higher temperatures in Nd_2Ni_2Sn and to lower temperatures in Tb_2Ni_2Sn. Finally, the peak disappears when the field is increased to 90 kOe, in both these cases, as shown in Figs. 5(a) and 5(b) for Nd_2Ni_2Sn and Tb_2Ni_2Sn. These variations suggest that the magnetic transition in Nd_2Ni_2Sn at T_2(=17 K)

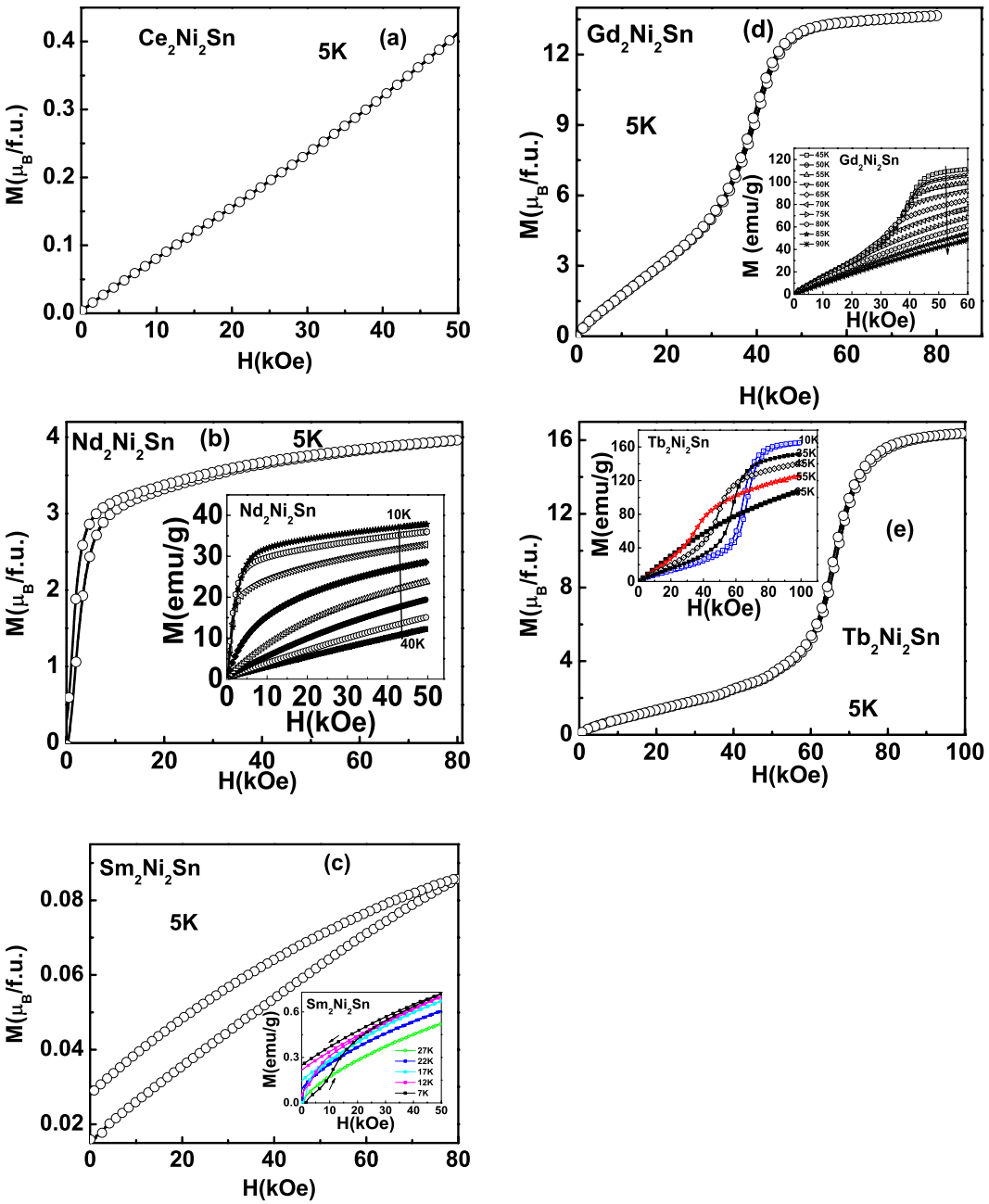

FIG. 3. (Color online) *M-H* isotherms of (a) Ce_2Ni_2Sn, (b) Nd_2Ni_2Sn, (c) Sm_2Ni_2Sn, (d) Gd_2Ni_2Sn, and (e) Tb_2Ni_2Sn at 5 K. The insets show the isotherms at higher temperatures.

is from ferromagnetic-paramagnetic, while that in Tb_2Ni_2Sn at T_1(=66) is from antiferromagnetic-paramagnetic, with an increase in temperature.[28,29] Heat capacity studies, therefore, support the observation made on the basis of the magnetization data.

The magnetic contribution to the heat capacity (C_M) of R_2Ni_2Sn [R=Ce, Nd, Sm, Gd, and Tb] has been determined from the heat capacity data. C_M was determined from the zero-field C-T by subtracting the nonmagnetic contribution from it. The nonmagnetic part of the heat capacity ($C_{\text{nonmagnetic}}$), which is the sum of the phonon (C_{ph}) and the electronic (C_e) contributions, was determined by using the following equation:[31]

$$C_{\text{nonmagnetic}} = C_e + C_{\text{ph}} = \gamma T + 9NR(T/\theta_D)^3 \int_0^{\theta_D/T} \frac{x^4 e^x}{(e^x - 1)^2} dx. \quad (1)$$

Here, N is the number of atoms per f.u. (N=5 in this case), R is the molar gas constant, γ is the electronic coefficient, and θ_D is the Debye temperature. From the fit at a low temperature using the equation,[31] namely, $C/T = \gamma + \beta T^2$, the values of the γ and $\theta_D = \sqrt[3]{12\pi^4 R/5\beta} \cong \sqrt[3]{1944/\beta}$[J/mol K] have been found out and are also given in Table III. It is found that the γ value for Gd_2Ni_2Sn is much larger compared to that in the other compounds of the series. However, this cannot be

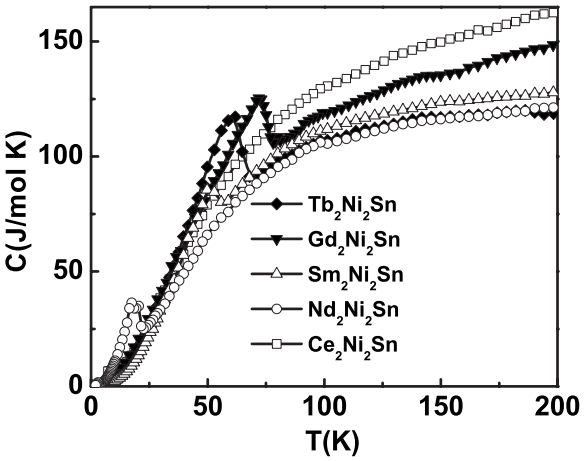

FIG. 4. Temperature variation of heat capacity of R_2Ni_2Sn compounds in zero field.

called a heavy fermion system due to the fact that the $4f$ shell of Gd is well localized. Similar unusually large values of γ have been reported in a few other Gd-based intermetallic compounds.[32–34] The reason for the enhancement of γ must be the short range correlations arising from the polarization of the Ni $3d$ band. The fact that the molecular field that is responsible for the polarization of the $3d$ band is large in Gd is responsible for the observation of the highest value of γ in the present series.

Figures 6(a)–6(d) show the temperature variation of the heat capacity of R_2Ni_2Sn compounds with R=Ce, Nd, Sm, Gd, and Tb, respectively. The calculated nonmagnetic contribution is also shown. The insets show the temperature variation of the magnetic contribution (C_M) and the magnetic entropy (S_M) of these compounds. The values of C_M and S_M at T^* are given in Table III.

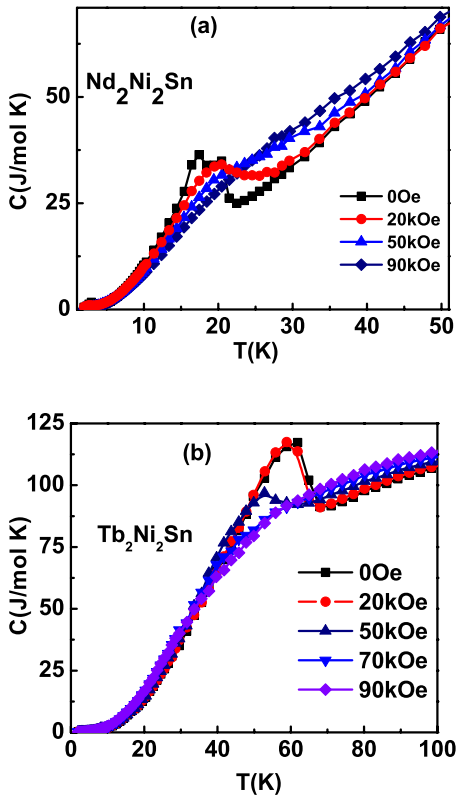

FIG. 5. (Color online) Temperature variation of heat capacity of (a) Nd_2Ni_2Sn and (b) Tb_2Ni_2Sn in different fields.

The value of C_M at T^* is about 16, 9, 14, and 27 J/mol K for Nd_2Ni_2Sn, Sm_2Ni_2Sn, Gd_2Ni_2Sn, and Tb_2Ni_2Sn, respectively. The magnetic entropy is calculated by using the relation $S_M(T)=\int(C_M(T)/T)dT$. From the insets of these figures, it is found that S_M at the highest temperature is less than the theoretical value $[R\ln(2J+1)]$ in all the cases, except Tb_2Ni_2Sn. Even in Gd_2Ni_2Sn, the difference between these two values is considerable, which implies that crystal field effect is not responsible for this behavior. We feel that the short range correlations of the induced moment on Ni are responsible for the entropy contribution at temperatures above T_1. The large difference seen in the case of Sm_2Ni_2Sn may be due to the admixture effect of the ground and excited multiplets.[30]

Among all the compounds studied, the magnetic contribution of the heat capacity of Sm_2Ni_2Sn shows a Schottky anomaly, as can be seen from Fig. 7. The Schottky contribution was fitted by using the following standard expression:[31]

$$C_M = \frac{R}{T^2}\left\{\frac{\sum_{i=1}^{3}\Delta_i^2 \exp\left[-\frac{\Delta_i}{T}\right]}{\sum_{i=1}^{3}\exp\left[-\frac{\Delta_i}{T}\right]} - \left[\frac{\sum_{i=1}^{3}\Delta_i \exp\left(-\frac{\Delta_i}{T}\right)}{\sum_{i=1}^{3}\exp\left(-\frac{\Delta_i}{T}\right)}\right]^2\right\}.$$

The corresponding CEF-split ground multiplet is also shown in Fig. 7. Each of these levels is a doublet, as expected for a Kramer ion such as Sm^{3+} (J=5/2).

The magnetocaloric effect of these compounds was determined in terms of isothermal magnetic entropy change as well as adiabatic temperature change by using Maxwell's equations.[35] The ΔS_M vs T plots of all these compounds, for field changes of 10–90 kOe, have been determined at various temperatures close to the transition temperatures. Figures 8(a)–8(d) show the temperature variation of the magnetic entropy change for Nd_2Ni_2Sn, Sm_2Ni_2Sn, Gd_2Ni_2Sn, and Tb_2Ni_2Sn, respectively.

It can be seen from these figures that ΔS_M vs T plots of all the compounds show a peak near T_1. However, no distinct peak associated with the transition at T_2 could be seen in these compounds, except in Tb_2Ni_2Sn. The fact that the magnetic moment of Sm_2Ni_2Sn is quite small compared to the other members of this series is responsible for the very low MCE values in this compound. Another feature worth noting from these plots is that the ΔS_M of these compounds does not die out even at temperatures well above the highest transition temperature. This trend is very pronounced in the case of Gd_2Ni_2Sn and can be attributed to the presence of short range magnetic correlations mentioned earlier. It can be seen from these figures that the $\Delta S_M^{\max}$ values, for ΔH=50 kOe, of Nd_2Ni_2Sn, Sm_2Ni_2Sn, Gd_2Ni_2Sn, and Tb_2Ni_2Sn compounds are ~7.2, 0.12, 4.6, and 2.8 J/kg K.

In contrast to the usual observation of a single MCE peak, in Tb_2Ni_2Sn and to a less extent in Gd_2Ni_2Sn, the temperature dependence of MCE is quite different. The entropy

TABLE III. Values of Debye temperature (θ_D), coefficient of electronic specific heat (γ), maximum values of magnetic heat capacity (C_M), and magnetic entropy (S_M) close to the transition temperature in R_2Ni_2Sn compounds.

Compound	θ_D (K)	γ (mJ/mol K^2)	$C_M(T^*)$ (J/mol K)/R^{3+} Expt.	$S_M(T^*)$ (J/mol K)/R^{3+} Expt.	$R\ln(2J+1)$ (J/mol K)
Nd_2Ni_2Sn	211	17	16	16	19.1
Sm_2Ni_2Sn	193	39	9	6	14.9
Gd_2Ni_2Sn	191	112	14	12	17.3
Tb_2Ni_2Sn	240	20	27	21	21.3

change is positive (negative MCE) below ~60 K and it changes its sign and becomes negative (positive MCE) at higher temperatures, giving rise to a distinguishable minimum (at T^{min}) and a maximum (at T^{max}) for all fields above 20 kOe. It is to be noted that while the temperatures corresponding to the minimum and zero entropy change shift to lower temperatures with field, the position of the maximum is almost insensitive to the field. This type of behavior can be analyzed in terms of the FM-AFM phase coexistence and the variation in the ratio of these phases under different applied fields. Table IV shows the maximum and minimum values of $(-\Delta S_M)$ with the corresponding temperatures and fields for Tb_2Ni_2Sn.

As evident from Fig. 8, at the lowest temperature, MCE is negligibly small and almost independent of the field. In the temperature range of T_2-T_3, the MCE is negative. This observation clearly indicates that the compound is predominantly antiferromagnetic in this region of temperature. When temperature is just above $T_N(=T_1)$, the MCE is positive and monotonically increases with field.

Figure 9 shows the ferromagnetic fraction as a function of temperature for several values of H. The ferromagnetic fraction has been calculated by subtracting the magnetization arising from the antiferromagnetic component (linear part of the magnetization isotherms) from the saturated magnetization values. The fraction of coexisting phases (AFM+FM)

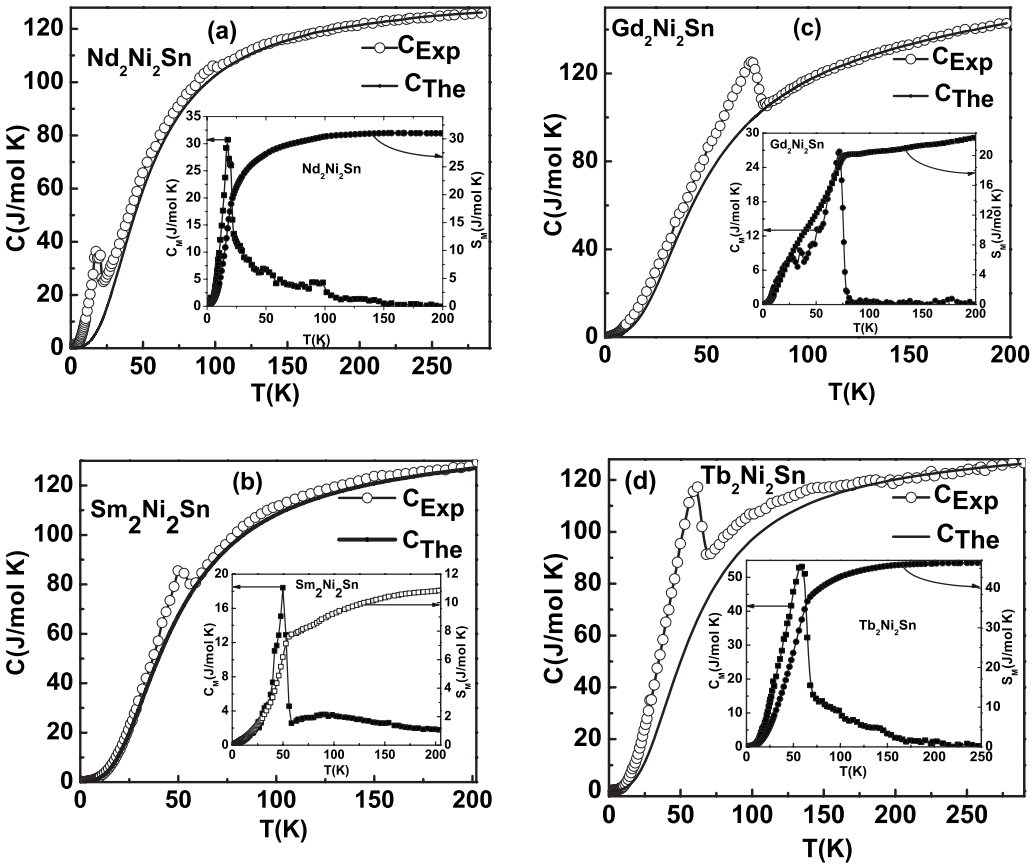

FIG. 6. Temperature variation of the heat capacity data (open circles) in (a) Nd_2Ni_2Sn, (b)Sm_2Ni_2Sn, (c) Gd_2Ni_2Sn, and (d) Tb_2Ni_2Sn. The calculated nonmagnetic contribution is shown by solid lines. The insets show the temperature dependence of the magnetic contribution (C_M) and zero-field magnetic entropy (S_M).

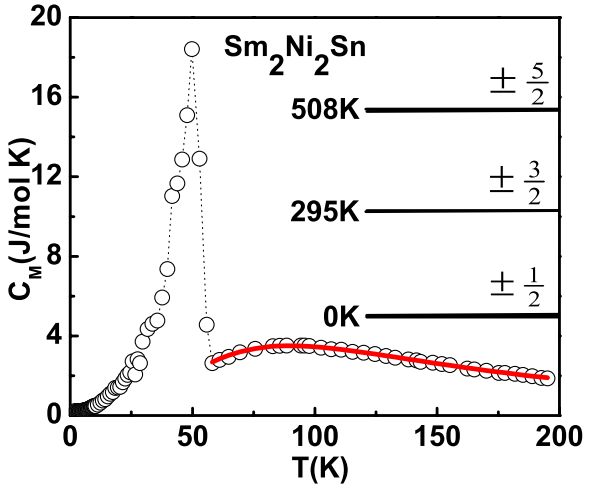

FIG. 7. (Color online) Temperature dependence of the magnetic part of the heat capacity showing the Schottky anomaly (shown in red) in Sm_2Ni_2Sn. The solid line represents the best fit of experimental data. The calculated splitting of the ground state multiplet by the crystal field is also shown.

can be controlled by H. In the $H \sim 20$ kOe case, the percentage of the AFM phase is considerable because this field is not sufficiently large to reach the onset of the metamagnetic transition. For higher fields, the FM fraction initially increases and then decreases near transition temperature. The insets of Figs. 9(a) and 9(b) show the temperature variation of first derivative of the ferromagnetic component (dM_{sat}/dt) as well as the isothermal magnetic entropy change calculated for 30 and 40 kOe for Gd_2Ni_2Sn and Tb_2Ni_2Sn, respectively.

TABLE IV. Maximum and minimum values of $(-\Delta S_M)$ along with the corresponding temperatures (T^{max} and T^{min}) and fields for Tb_2Ni_2Sn.

H (kOe)	T^{max} (K)	$-\Delta S_M^{max}$ (J/kg K)	T^{min} (K)	$-\Delta S_M^{min}$ (J/kg K)
20	68.9	0.9	57.5	−1.1
50	68.7	2.2	52.2	−5.0
70	67.6	4.5	39.5	−6.4
90	67.3	7.2	37.2	−6.0

It is quite evident that these two variations are correlated. Furthermore, comparison of Figs. 8 and 9 shows that the MCE minima and maxima correspond to the points of inflection of the increasing and decreasing parts of the curve showing the ferromagnetic fraction, respectively. This feature is in agreement with the prediction of Tishin and Spichkin.[35] The increasing part of these curves reflects the dominance of the Zeeman energy over the thermal energy, while the decreasing portion of this curve shows the reversed scenario. Further increasing tendency seen in the ferromagnetic fraction at high temperatures is due to the paramagnetic contribution as this temperature range is above $T_N(=T_1)$.

Results obtained on the magnetic and magnetocaloric effects, particularly in Tb_2Ni_2Sn, show some striking similarities with those seen in $(Pr,Ca)MnO_3$ manganite system recently reported by Gomes *et al.*[36] Both these systems show the coexistence of antiferromagnetic and ferromagnetic components in the low temperature range. As a consequence, in both these systems, the sign of MCE changes from negative

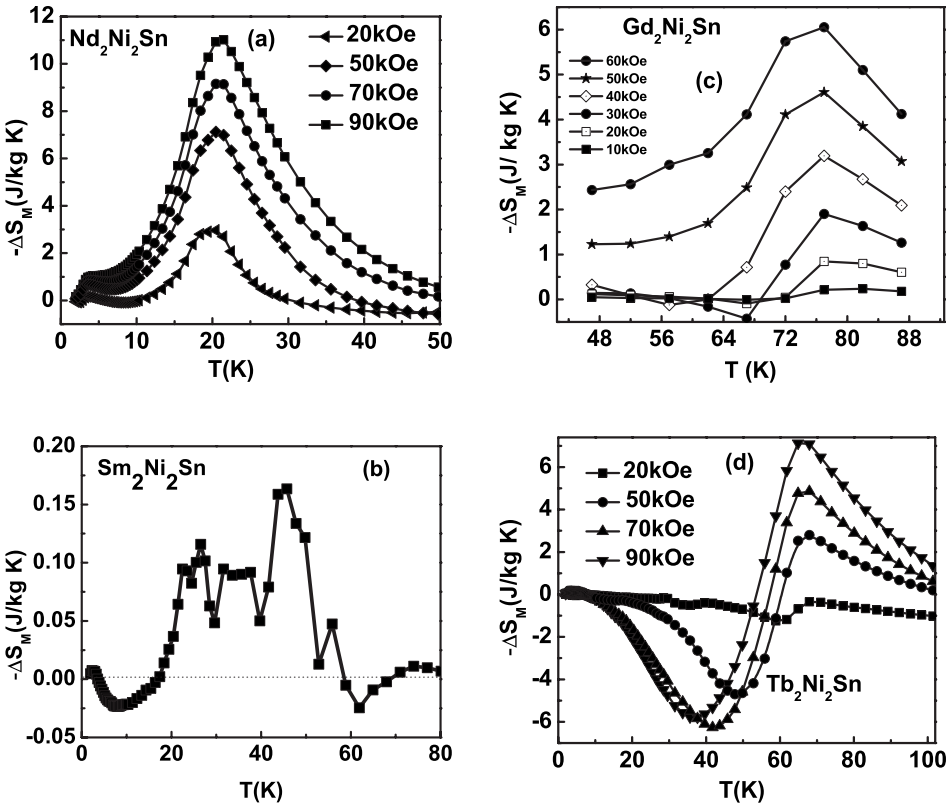

FIG. 8. Temperature variation of the isothermal magnetic entropy change in (a) Nd_2Ni_2Sn, (b) Sm_2Ni_2Sn, (c) Gd_2Ni_2Sn, and (d) Tb_2Ni_2Sn for various field changes.

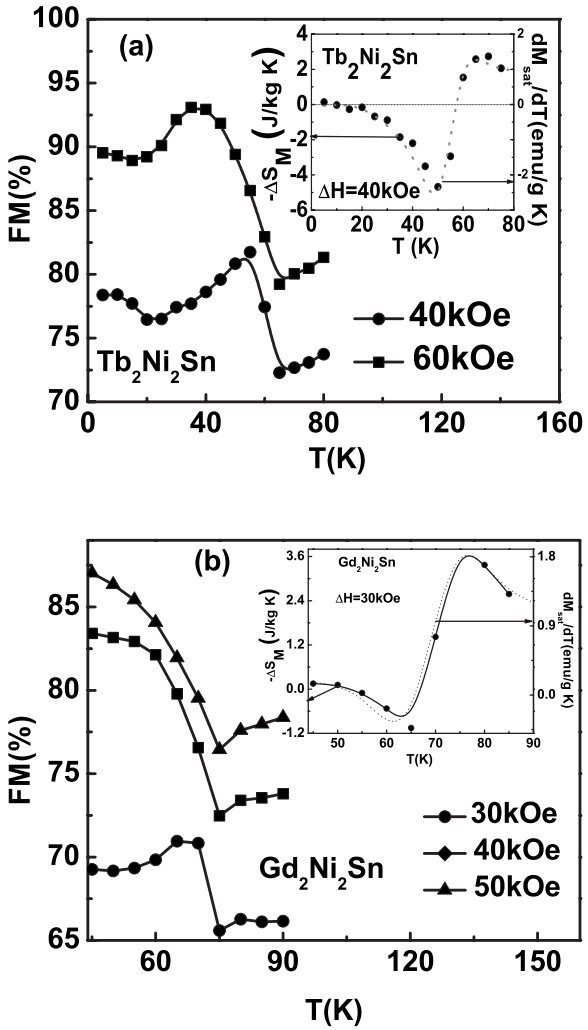

FIG. 9. Ferromagnetic fraction as a function of temperature for different applied fields in (a) Tb_2Ni_2Sn and (b) Gd_2Ni_2Sn compounds. The insets show the comparison between $-\Delta S_M$ and the first derivative of the ferromagnetic component for a field of 30 kOe in Gd_2Ni_2Sn and 40 kOe in Tb_2Ni_2Sn.

to positive as the temperature is increased. Furthermore, the temperature variation of magnetic entropy change is closely related to the change in the ferromagnetic fraction. It has been suggested that the anomalous MCE behavior in $(Pr,Ca)MnO_3$ is due to the presence of successive ferromagnetic and antiferromagnetic slabs in the unit cell. von Ranke *et al.*[37] showed that the MCE in $DyAl_2$ single crystals show a similar negative to positive change over behavior, which was attributed to the metamagnetic transition. Very recently, a similar MCE behavior has been reported in $Ce(Fe,Ru)_2$ compounds, which is explained on the basis of the coexisting FM and AFM phases.[38] Based on the magnetic and neutron diffraction studies in Dy_2Ni_2Sn, which is isostructural to Gd_2Ni_2Sn and Tb_2Ni_2Sn, Penc *et al.*[21] showed that the low temperature magnetic structure of this compound is noncollinear with large AFM and small FM components. The FM component is along the *a* axis, while the AFM component is in the *ac* plane. These studies have also shown that Ni is nonmagnetic in this compound. The magnetic transitions seen in these compounds arise due to the anisotropic exchange interactions. The anisotropy arises from the considerably different intraplanar and interplanar *R*-*R* bond lengths. Therefore, it is probable that the *R* sublattice in Tb_2Ni_2Sn resembles that of $(Pr,Ca)MnO_3$ with different types of magnetic order within and between the layers in the unit cell. The fact that strong antiferromagnetic component exists only in Tb_2Ni_2Sn, as revealed by a negative θ_P value, is in agreement with the peculiar MCE behavior seen predominantly only in this compound.

The temperature variation of the adiabatic temperature change has also been calculated for Nd_2Ni_2Sn, Sm_2Ni_2Sn, Gd_2Ni_2Sn, and Tb_2Ni_2Sn. In all the compounds, ΔT_{ad} was determined by using the *C*-*H*-*T* data. The ΔT_{ad} vs *T* plots of all the compounds are shown in Figs. 10(a)–10(d). It can be seen from these figures that the temperature variation of ΔT_{ad} is almost identical to that of ΔS_M. Table V shows the transition temperature (T_1), isothermal magnetic entropy change, and the adiabatic temperature change for a field change of 50 kOe in R_2Ni_2Sn compounds. The ΔT_{ad}^{max} value of GdPd, which is an active magnetic regenerator material used at the low temperature stage of practical magnetic refrigerators for liquefaction of hydrogen, is 8.7 K for a field change of 70 kOe.[39] Therefore, a comparison of the ΔT_{ad}^{max} values of some of the members of the present series with that of the potential refrigerant materials indicates that these materials may find applications as magnetic refrigerants at low temperatures. Another interesting aspect particularly seen in Tb_2Ni_2Sn is the oscillatory magnetocaloric behavior. The large negative MCE shown by this compound makes this an attractive candidate for heat pumps based on MCE.

In the light of the interesting magnetocaloric behavior seen in R_2Ni_2Sn compounds, the electrical resistivity measurements of these compounds both in zero field and in applied fields have been carried out. Using this, the MR was calculated. MR could not be measured in Gd_2Ni_2Sn and Tb_2Ni_2Sn, as the sample was flying off the puck when the field was turned on. The temperature dependence of electrical resistivity for all the compounds is shown in Fig. 11. All the compounds show a metallic behavior. It may also be noticed from the figure that there is a change in the slope of the resistivity near the magnetic transition temperature (T_1) in most of the compounds. However, no anomaly corresponding to the low temperature (T_2 and T_3) could be seen in any of the compounds. In the case of Ce_2Ni_2Sn, the slope change occurs at a temperature well above T_1. Though the electrical resistivity of Ce_2Ni_2Sn has been investigated in

TABLE V. Transition temperature, maximum values of isothermal magnetic entropy change, and the adiabatic temperature change for a field change of 50 kOe in R_2Ni_2Sn compounds.

Compound	T_1 (K)	$(\Delta S_M)^{max}$ (J/kg K)	ΔT_{ad}^{max} (K)
Nd_2Ni_2Sn	22	7.2	2.5
Sm_2Ni_2Sn	50	0.1	0.1
Gd_2Ni_2Sn	75	4.6	1.4
Tb_2Ni_2Sn	66	2.9	2.8

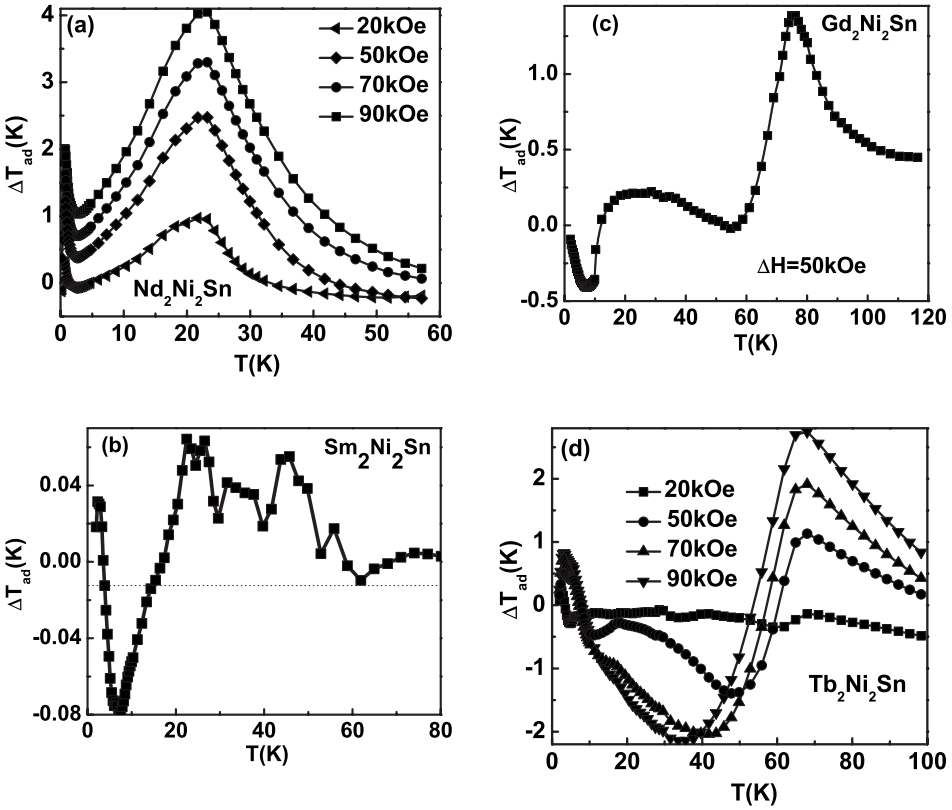

FIG. 10. Temperature dependence of adiabatic temperature change of (a) Nd_2Ni_2Sn, (b) Sm_2Ni_2Sn, (c) Gd_2Ni_2Sn, and (d) Tb_2Ni_2Sn in different fields.

some detail,[27,40,41] there seems to be no agreement among these reports. It has been reported that this compound shows Kondo effect at low temperature. The results obtained in the present work are found to be very similar to the observations reported by Fourgeot *et al.*,[40] although in the present case, the drop in the resistivity starts at higher temperatures, on cooling. It should be emphasized here that the magnetic transition temperature reported by these authors are in very good agreement with the present data.

In all the cases except Ce_2Ni_2Sn, the resistivity is found to follow $\rho=\rho_0+AT^2$ behavior at low temperatures and $\rho=\rho_0+BT-CT^3$ behavior at temperatures above T_1. Here, ρ_0 is the residual resistivity and A, B, and C are temperature independent constants.[42–44] Values of A [in the range of $(1-10)\times10^{-5}$ mΩ cm/K^2] suggest that the electron spin-wave scattering is the dominant factor in determining the electrical resistivity in the temperature range. The fact that the data at high temperatures fit well to the relation $\rho=\rho_0+BT-CT^3$ indicates that the phonon contribution and the *s-d* scattering are crucial in this temperature regime.

The magnetoresistance defined as $\Delta\rho/\rho(\%)=[\rho(H)-\rho(0)]/\rho(0)\times100$ for Ce_2Ni_2Sn and Nd_2Ni_2Sn compounds has been studied in various temperature regions, as shown in Fig. 12. It can be seen from this figure that the MR for

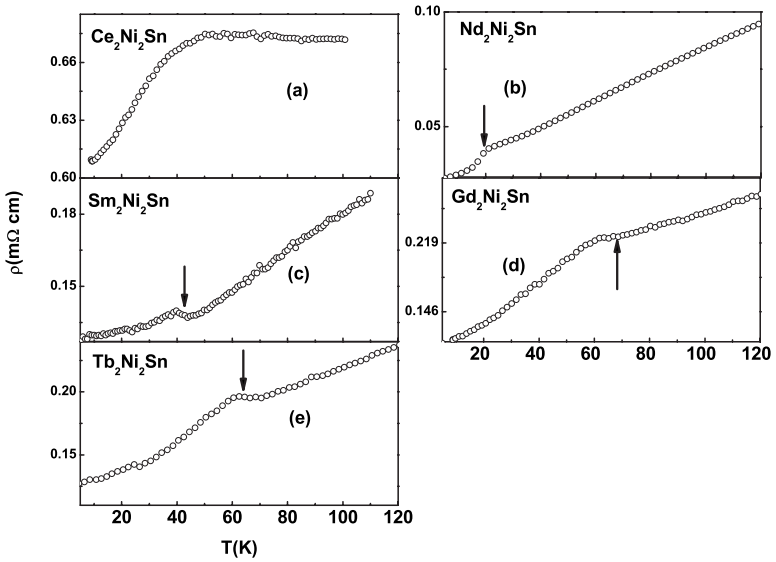

FIG. 11. Temperature dependence of electrical resistivity of (a) Ce_2Ni_2Sn, (b) Nd_2Ni_2Sn, (c) Sm_2Ni_2Sn, (d) Gd_2Ni_2Sn, and (e) Tb_2Ni_2Sn compounds. The arrow indicates the transition temperature seen from these plots.

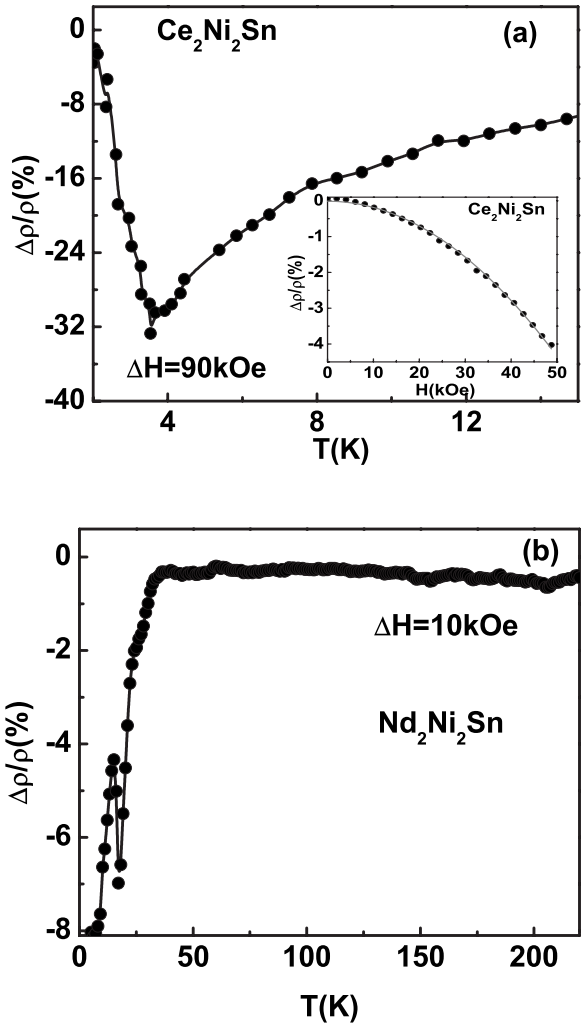

FIG. 12. Temperature dependence of magnetoresistance of (a) Ce_2Ni_2Sn and (b) Nd_2Ni_2Sn compounds. The filled circles show the experimental data and the line shows the fitted data. The inset of (a) shows the variation of magnetoresistance with field at 8 K.

Ce_2Ni_2Sn and Nd_2Ni_2Sn is negative in the entire temperature range. It may be seen from Fig. 12(a) that the MR at transition temperature (T_1) and for a field change of 90 kOe is negative with a magnitude of about 32%. Chevalier *et al.*[41] reported about 20% negative MR at 6 K for a field of 90 kOe, which is in very good agreement with the present data. These authors also reported that below 5 K, the sign of MR becomes positive. However, in the present case, although the magnitude of MR decreases below 4 K, it retains the negative sign down to the lowest temperature. The unusually large MR in this compound may be attributed to the Kondo effect.[45] It is also reasonable to assume that the Kondo effect is the major factor in determining the sign of the MR. Similar MR behavior was reported in other Kondo systems such as $CeNi_{1-x}Cu_x$.[46] The inset of Fig. 12(a) shows the field variation of magnetoresistance. The quadratic dependence of MR on the field, as seen from the figure, is indicative of the presence of spin fluctuations.[47] Based on the magnetization data, Fourgeot *et al.*[24] reported that Ce_2Ni_2Sn shows characteristics of heavy fermion systems. They also suggested that the broad peak in the M-T data around 8 K is a result of the spin fluctuations arising from the Kondo effect. In the case of Nd_2Ni_2Sn, the MR turns negative below T_1 even for a small field of 10 kOe. It can be seen from Fig. 12(b) that the MR starts increasing at temperatures close to T_1, attaining a maximum value of 7% as the temperature is reduced. The trend reverses at temperatures close to T_2, at which the MR starts decreasing and finally attains the maximum value of about 8% at the lowest temperature. The negative MR in this compound must be associated with the weak antiferromagnetic component present at low temperatures.[22]

IV. CONCLUSIONS

Magnetization measurements carried out in various R_2Ni_2Sn compounds have revealed that the magnetic state of these compounds are complex. Simultaneous existence of ferromagnetic and antiferromagnetic orders is found in most of the compounds, although in varying degrees. These competing interactions are found to result in multiple magnetic transitions. The magnetization is not found to saturate even at a field of 100 kOe, probably due to the canted structure. Although the high temperature susceptibility obeys the Curie–Weiss law, the sign of the paramagnetic Curie temperature seems to be in conflict with the M-T behavior, except in Tb_2Ni_2Sn. Analysis of the zero-field heat capacity data shows that the magnetic entropy is less than the theoretical value, indicating the presence of some moment on Ni. Schottky anomaly is present in the magnetic heat capacity data of Sm_2Ni_2Sn. The temperature variation of magnetocaloric effect reflects the temperature variation of the magnetization behavior. Tb_2Ni_2Sn shows oscillatory magnetocaloric effect, which may be of great interest in applications based on MCE. The MCE variation in this compound has been correlated with the ferromagnetic-antiferromagnetic phase coexistence. The electrical resistivity analysis has shown that the electron-magnon scattering is prominent at low temperature, while s-d scattering is crucial at high temperatures. The magnetoresistance is very large in Ce_2Ni_2Sn and shows a quadratic dependence on the field, implying the role of spin fluctuations in determining the electrical resistivity and MR. Large MR has been observed in other compounds of this series as well.

ACKNOWLEDGMENT

One of the authors (K.G.S.) thanks ISRO, Government of India, for providing financial support for this work

*Also at Ames Laboratory, Iowa State University, Ames, IA 50011.
†Corresponding author. suresh@phy.iitb.ac.in

[1] V. K. Pecharsky and K. A. Gschneidner, Jr., J. Magn. Magn. Mater. **200**, 44 (1999).
[2] V. K. Pecharsky and K. A. Gschneidner, Jr., Phys. Rev. Lett. **78**, 4494 (1997).
[3] Proceedings of the First International Conference on Magnetic Refrigeration at Room Temperature, edited by P. W. Egolf, (International Institute of Refrigeration, Paris, France, 2005).
[4] Proceedings of the Second International Conference on Magnetic Refrigeration at Room Temperature, edited by A. Poredos and A. Sarlah, (International Institute of Refrigeration, Paris, France, 2007).
[5] N. K. Singh, S. Agarwal, K. G. Suresh, R. Nirmala, A. K. Nigam, and S. K. Malik, Phys. Rev. B **72**, 014452 (2005).
[6] K. A. Gschneidner, Jr. and V. K. Pecharsky, Mater. Sci. Eng., A **287**, 301 (2000).
[7] P. Kumar, N. K. Singh, K. G. Suresh, and A. K. Nigam, J. Alloys Compd. **427**, 42 (2007).
[8] P. Kumar, N. K. Singh, K. G. Suresh, A. K. Nigam, and S. K. Malik, J. Appl. Phys. **101**, 013908 (2007).
[9] V. K. Pecharsky and K. A. Gschneidner, Jr., Phys. Rev. Lett. **78**, 4494 (1997).
[10] W. Choe, V. K. Pecharsky, A. O. Pecharsky, K. A. Gschneidner, Jr., V. G. Young, Jr., and G. J. Miller, Phys. Rev. Lett. **84**, 4617 (2000).
[11] K. A. Gschneidner, Jr., V. K. Pecharsky, E. Brück, H. G. M. Duijn, and E. M. Levin, Phys. Rev. Lett. **85**, 4190 (2000).
[12] A. Fujita, S. Fujieda, Y. Hasegawa, and K. Fukamichi, Phys. Rev. B **67**, 104416 (2003).
[13] S. Gama, A. A. Coelho, A. de Campos, A. M. Carvalho, F. C. G. Gandra, P. J. von Ranke, and N. A. de Oliveira, Phys. Rev. Lett. **93**, 237202 (2004).
[14] H. Wada and Y. Tanabe, Appl. Phys. Lett. **79**, 3302 (2001).
[15] O. Tegus, E. Bruck, K. H. J. Buschow, and F. R. de Boer, Nature (London) **415**, 150 (2002).
[16] N. K. Singh, K. G. Suresh, A. K. Nigam, S. K. Malik, A. A. Coelho, and S. Gama. J. Magn. Magn. Mater. **317**, 68 (2007).
[17] N. K. Singh, P. Kumar, K. G. Suresh, A. K. Nigam, A. A Coelho, and S. Gama, J. Phys.: Condens. Matter **19**, 036213 (2007).
[18] A. Planesa, Ll. Manosa, X. Moya, T. Krenke, M. Acet, and E. F. Wassermann, Solid State Commun. **310**, 2767 (2007).
[19] M. H. Phan and S. C. Yu, J. Magn. Magn. Mater. **308**, 325 (2007).
[20] R. P. Pinto, M. M. Amado, M. E. Braga, Yu. G. Pogorelov, B. Chevalier, J. Étourneau, and J. B. Sousa, J. Magn. Magn. Mater. **196-197**, 710 (1999).
[21] B. Penc, M. Hofmann, M. Slaski, P. Starowicz, and A. Szytula, J. Alloys Compd. **282**, 8 (1999).
[22] B. Chevalier, F. Fourgeot, L. Fournès, P. Gravereau, G. Le Caër, and J. Etourneau, Physica B (Amsterdam) **226**, 283 (1996).
[23] B. Chevalier, F. Fourgeot, D. Laffargue, P. Gravereau, L. Fournès, and J. Etourneau, J. Alloys Compd. **262-263**, 114 (1997).
[24] F. Fourgeot, B. Chevalier, P. Gravereau, L. Fournès, and J. Etourneau, J. Alloys Compd. **218**, 90 (1995).
[25] D. Laffargue, F. Bourée, B. Chevalier, J. Etourneau, and T. Roisnel, Physica B (Amsterdam) **259-261**, 46 (1999).
[26] R. P. Pinto, M. M. Amado, M. E. Braga, J. B. Sousa, B. Chevalier, D. Laffargue, and J. Étourneau, J. Appl. Phys. **79**, 6355 (1996).
[27] R. A. Gordon, Y. Ijiri, C. M. Spencer, and F. J. DiSalvo, J. Alloys Compd. **224**, 101 (1995).
[28] N. K. Singh, K. G. Suresh, R. Nirmala, A. K. Nigam, and S. K. Malik, J. Appl. Phys. **101**, 093904 (2007).
[29] N. K. Singh, K. G. Suresh, R. Nirmala, A. K. Nigam, and S. K. Malik, J. Appl. Phys. **99**, 08K904 (2006).
[30] K. H. J. Buschow, *Handbook of Magnetic Materials* (Elsevier, Amsterdam, 1999), Vol. 12.
[31] E. S. R. Gopal, *Specific Heat at Low Temperatures* (Plenum, New York, 1976).
[32] R. Mallik, P. L. Paulose, E. V. Sampathkumaran, S. Patil, and V. Nagarajan, Phys. Rev. B **55**, 8369 (1997).
[33] E. V. Sampathkumaran and I. Das, Physica B (Amsterdam) **223-224**, 149 (1996).
[34] M. J. Parsons, J. Crangle, K. U. Neumann, and K. R. A. Ziebeck, J. Magn. Magn. Mater. **184**, 184 (1998).
[35] A. M. Tishin and Y. I. Spichkin, *The Magnetocaloric Effect and Its Applications* (IOP, Bristol, 2003).
[36] A. M. Gomes, F. Garcia, A. P. Guimarães, M. S. Reis, and V. S. Amaral, Appl. Phys. Lett. **85**, 4974 (2004).
[37] P. J. von Ranke, I. G. de Oliveira, A. P. Guimaraes, and X. A. da Silva, Phys. Rev. B **61**, 447 (2000).
[38] M. K. Chattopadhyay, M. A. Manekar, and S. B. Roy, J. Phys. D **39**, 1006 (2006).
[39] A. M. Tishin, K. A. Gschneidner, Jr., and V. K. Pecharsky, Phys. Rev. B **59**, 503 (1999).
[40] F. Fourgeot, B. Chevalier, P. Gravereau, L. Fournès, and J. Etourneau, J. Alloys Compd. **218**, 46 (1999).
[41] B. Chevalier, J. G. Soldevilla, J. C. G. Sal, J. M. Barandiaràn, and J. Etourneau, J. Magn. Magn. Mater. **196-197**, 878 (1999).
[42] E. Gratz and M. J. Zuckermann, in *Handbook on the Physics and Chemistry of Rare Earths*, edited by K. A. Gschneidner, Jr. and L. Eyring, (North Holland Publishing Company, Amsterdam, 1982).
[43] I. A. Campbell and A. Fert, in *Ferromagnetic Materials*, edited by E. P. Wohlfarth, (North Holland Publishing Company, Amsterdam, 1982), Vol. 3.
[44] K. G. Suresh and K. V. S. Rama Rao, J. Alloys Compd. **238**, 90 (1996).
[45] V. V. Gridin, S. A. Sergeenkov, A. M. Strydom, and P. V. du Plessis, Phys. Rev. B **50**, 12995 (1994).
[46] J. G. Soldevilla, J. C. G. Sal, J. R. Fernandez, J. I. Espeso, and J. A. Balnco, Physica B **259-261**, 38 (1999).
[47] R. Rawat and I. Das, J. Phys.: Condens. Matter **13**, L379 (2001).